

Thermoelectric properties of Co-doped BiFeO₃ and Bi₂₄CoO₃₇-BiFeO₃ compound systems

Takeshi YOKOTA,[†] Rintaro AOYAGI* and Manabu GOMI

Department of Materials Science and Engineering, Graduate School of Nagoya Institute of Technology, Gokiso-cho, Showa-ku, Nagoya 466-8555, Japan

*Department of Mechanics, Energy, Fine Measurements, and Electronics, Graduate School of Nagoya Institute of Technology, Gokiso-cho, Showa-ku, Nagoya 466-8555, Japan

We investigated the thermoelectric properties of doped multiferroic material: Co-doped BiFeO₃ (BFO) and related materials: Bi₂₄CoO₃₇ and Bi₂₄CoO₃₇-BFO composite systems. Because of their insulating nature, the BFO-based samples showed high Seebeck coefficients compared with other oxides being explored as candidates for new thermoelectric materials such as NaCo₂O₄, and La_{0.9}Sr_{0.99}Ca_{0.11}CoO₄. On the other hand, the Bi₂₄CoO₃₇ sample showed high conductivity. The Bi₂₄CoO₃₇ (20%)–BFO composite sample showed a high power factor, because of its high conductivity and high Seebeck coefficient. These results indicated that the BFO matrix plays an important role in maintaining a high Seebeck coefficient, and that Bi₂₄CoO₃₇ works as a conductive pass on this system.

©2013 The Ceramic Society of Japan. All rights reserved.

Key-words : High temperature thermoelectric properties, Seebeck coefficient, Multiferroic materials, Composite, Valence fluctuation

[Received April 16, 2013; Accepted June 27, 2013]

1. Introduction

Given the increasingly urgent need for new forms of clean energy, the conversion of heat energy to electric energy using thermoelectric materials has received much attention. Although thermoelectric materials are important candidates for new energy sources, there are still issues concerning their low conversion efficiency. This issue is due to difficulties in increasing the thermoelectric figure of merit $ZT = S^2\sigma/\kappa$, with S being the Seebeck coefficient, κ the thermal conductivity and σ the conductivity. To improve the performance of thermoelectric materials, it is necessary to control the lattice thermal conductivity and for the material to have a high electrical conductivity. However the thermal conductivity has contributions from both electrons (k_e) and phonons (k_p). Therefore, high electrical conductivity greatly increases electron thermal conductivity. Regarding this issue, several oxide materials, specifically perovskite manganese oxides and layered cobaltite, have been investigated and proposed as potential candidates for thermoelectric applications.^{1)–9)} These oxides shows thermo power comparable to that of the traditional low-carrier-concentration thermoelectric alloys. In particular, manganese oxide has successfully undergone high electron doping and shown good thermoelectric performance. Based on these essential researches, we focused on a multiferroic material, BiFeO₃, as a candidate high-temperature thermoelectric material, because the material's leakage current mechanism has unique characteristics.¹⁰⁾ The specific domain wall, which is along the 109 and 180° domain, is responsible for its leakage current mechanism. This could be an advantage for thermoelectric properties, because the current pass anisotropy, such as a current flowing along the domain wall, is naturally similar to the granular

structure, which should have a low lattice thermal conductivity and a high electrical conductivity. In addition to that, since BFO is multiferroic,¹¹⁾ it should have a long-range magnetic order, which is typically accompanied by high conductivity. In this study, we mainly investigated the thermoelectric properties of Co-doped BiFeO₃ bulk ceramics. Since the magnetism of BiFeO₃ originates from the d-orbital of Fe, we speculated that we could change the magnetic order of BiFeO₃ by doping the transition metal, allowing it high conductivity without increasing the lattice thermal conductivity, mentioned above as the multiferroic feature. We also investigated Bi₂₄CoO₃₇ and the Bi₂₄CoO₃₇-BiFeO₃ composite system, because Bi₂₄CoO₃₇, which is Co silenite, is usually precipitated on high Co-doped BiFeO₃ samples.

2. Experimental procedure

Co-doped BiFeO₃ samples were prepared by solid-state reaction. The starting materials were high-purity (3N) powders of Bi₂O₃, Fe₂O₃ and Co₃O₄. To avoid Bi vacancies, 10% La was doped into the sample. Then, we prepared the samples, namely, (Bi_{0.9}La_{0.1})(Fe_{1-x}Co_x)O₃ [$x = 0, 0.05, 0.10$]. (Bi_{0.9}La_{0.1})FeO₃ is renamed as a BFO. We also prepared Bi₂₄CoO₃₇ and a Bi₂₄CoO₃₇-(Bi_{0.9}La_{0.1})FeO₃ (BFO) composite. For the compositions of 10 and 20 vol % Bi₂₄CoO₃₇ was used. After weighing, the powders were ball-milled with ethanol for 24 h. Then, the mixtures were dried and calcined in air at 1003 K for 12 h. After calcination, the powders were reground with ethanol in a ball mill for 24 h and pressed into pellets ($\phi 13 \times 3$ mm). Finally, these pellets were sintered in air at 1073 K for 12 h. The densities of the samples were measured using Archimedes' Principle. Structural analysis of the samples was performed using an X-ray diffractometer (XRD) employing Cu K α radiation. Conductivity and the Seebeck coefficient were measured in air by the four-probe method using the Thermoelectric Properties Measurement System (Ozawa Science, MODEL 2001i).

[†] Corresponding author: T. Yokota; E-mail: yokota.takeshi@nitech.ac.jp

3. Results and discussion

The relative density of all samples except pure BFO was about 90%. The relative density of BFO was about 86%. **Figure 1** shows XRD patterns of the samples. All diffraction patterns were identified as BFO or Bi₂₄CoO₃₇. Since Bi₂₄CoO₃₇ was observed in the XRD patterns of Co-doped BFO samples, we know that not all Co is substitutionally dissolved into BFO. The inset of Fig. 1 shows an enlarged view around the angle from 31 to 34° of the Co-doped BFO. It is clear that the diffraction patterns were shifted to a negative diffraction angle compared with undoped BFO. The peak shift of the Co-doped (5%) sample was larger than that of the Co-doped (10%) sample. This may be explained by the existence of the Bi₂₄CoO₃₇ precipitation or a magnetic agglutination for reducing a binding energy.^{12),13)} From these results, there is a solid solubility limitation below 5%. Although Bi₂₄CoO₃₇ precipitation was observed in all Co-doped samples, it was revealed that some of the Co should be dissolved into the BiFeO₃ matrix from this peak shift. We also estimated the lattice parameter of the Co-doped samples from the diffraction patterns. The *a*-axis values of BFO and Co-doped BFO (5 and 10%) were about 5.5730, 5.5821, and 5.5793 Å. The *c*-axis values of BFO and Co-doped BFO (5 and 10%) were about 13.8274, 13.8542, and 13.844 Å. The Fe site in BFO has 6 coordinates. In addition to that, Lyubutin et. al. found that the Fe spin state of ferromagnetic BiFeO₃ is high.¹⁴⁾ In fact, our sample showed hysteresis in its magnetization curve. Therefore, Fe should exist as a high spin state with a valence state of 3+ or 2+. Taking into account the coordination, the Fe spin state, and Shannon's effective ionic radius, Fe (3+) and Fe (2+) would be 0.645 and 0.78 Å, respectively.¹⁵⁾ Co also exists as a high spin state in BiCoO₃.¹⁶⁾ If Co exists as a Co³⁺ (0.61 Å), the d-spacing would not be expanded. Therefore, Co should exist as Co (2+) with a high spin state in the BFO lattice.

Figure 2 shows the conductivity of those samples. The undoped BFO showed constant conductivity against measure-

ment temperatures. The Co-doped sample showed high conductivity compared with the undoped samples above 735 K. However, the conductivity was barely changed with increases in Co content. This means that the amount of Co had already reached the solid solubility limitation. Therefore, the conductivity doesn't change further with the increased Co concentration. From the results of XRD patterns, Co could exist as a valence state of 2+. But with the increases of the Co content, the diffraction patterns shifts became smaller. We are still under investigating the origin of the relationship between the lattice change and conductivity. The Bi₂₄CoO₃₇ sample showed the highest conductivity among the samples. The composite samples showed lower conductivity than the undoped BFO sample. The conductivity increased with the increase of the amount of Bi₂₄CoO₃₇. Since the thermal activation energy (*E_a*) of each composite sample estimated using Arrhenius plots is about 0.66 eV, the origin of the carrier in those samples should be the same. However, the conductivity behavior of composite samples is not the same as the combined conductivity with silenite (*E_a* = 0.92 eV) and BFO (*E_a* = 0.18 eV). Therefore, a different impurity state from silenite or BFO was formed in the composite sample. Although no other diffraction pattern except those of silenite and BFO was observed in the XRD patterns, this could originated from the intermediate phase between Silenite and BFO interface due to inter-diffusion.¹⁷⁾

Figure 3 shows Seebeck coefficient of those samples. All sample showed positive sign in Seebeck coefficient. This means majority carrier of those samples is p-type. In the case of BFO, Bi vacancies are responsible for this conduction type.¹⁸⁾ Most of samples showed high Seebeck coefficient except Bi₂₄CoO₃₇

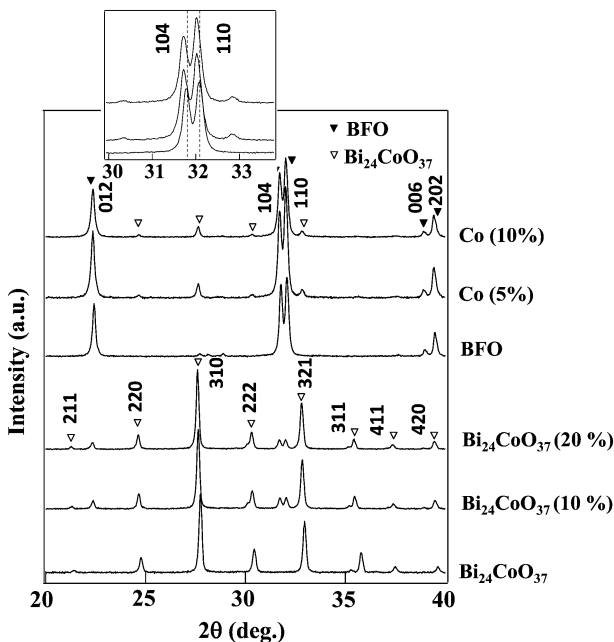


Fig. 1. X-ray diffraction patterns of the Co-doped (0, 5, 10%) BiFeO₃, Bi₂₄CoO₃₇ and Bi₂₄CoO₃₇ (10, 20%)–BFO composite system. Inset showed enlarged view of the Co-doped sample at around 30–34°.

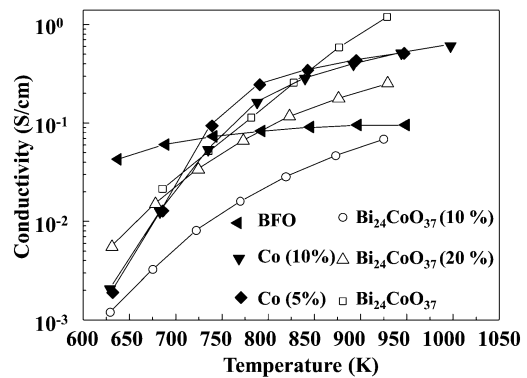


Fig. 2. Electrical conductivity of the Co-doped (0, 5, 10%) BiFeO₃, Bi₂₄CoO₃₇ and Bi₂₄CoO₃₇ (10, 20%)–BFO composite system.

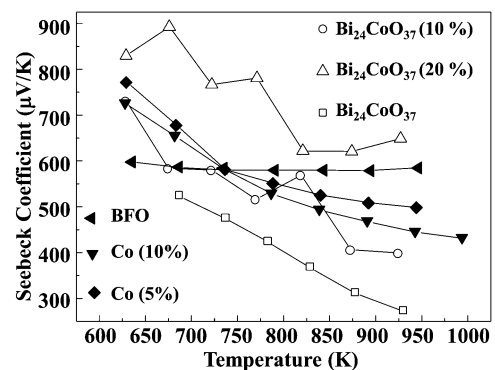


Fig. 3. Seebeck coefficient of the Co-doped (0, 5, 10%) BiFeO₃, Bi₂₄CoO₃₇ and Bi₂₄CoO₃₇ (10, 20%)–BFO composite system.

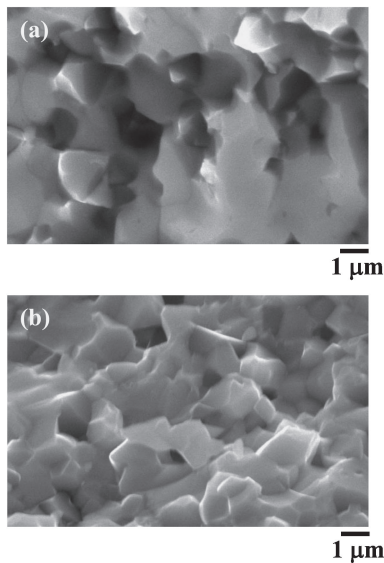


Fig. 4. SEM images of the sample of (a) $\text{Bi}_{24}\text{CoO}_{37}$ (10%)–BFO and (b) $\text{Bi}_{24}\text{CoO}_{37}$ (20%)–BFO composite system. Accelerate voltage is 30 kV. Magnification is 10,000.

compared with other oxide as a candidate of new thermoelectric materials such as NaCo_2O_4 , and $\text{La}_{0.9}\text{Sr}_{0.99}\text{Ca}_{0.11}\text{CoO}_4$. It is more likely due to its insulating nature of BFO matrix, which is low electric thermal conductivity. The Seebeck coefficient decrease with the increase of the temperature. This behavior is opposite tendency, which is explained by following equation as shown in Eq. (1).

$$S = k/e\{\ln(N/c) + A\} \quad (1)$$

k : Boltzman constant, A is a constant, and N is the effective density of state.

The effective density of state can be expressed by Eq. (2)

$$N = 2(2\pi m_e kT/h^2)^{3/2} \quad (2)$$

where m_e is the electron effective mass, h is the Plank constant, and T is the temperature. Although the relationship by which conductivity increases and Seebeck coefficient decreases is explained by the above equation, this tendency differs depending on the sample. For example, the conductivity of the 10% composite sample is lower than that of the 20% composite sample. However, the Seebeck coefficient is opposite. One possible reason is its composite structure. Since the matrix of the sample is BFO, the electric thermal conductivity should be low. Even when the structural advantage is taken into account, the reason for the high Seebeck coefficient of the 20% composite sample is still unclear. **Figure 4** shows SEM images of the 10 and 20% composite samples. There is no significant difference between the two samples. To emphasize the point, the micro structure of the 10% sample seems to be melting. Although we are still investigating the details of this behavior, the existence of grain boundary in the 20% composite sample might assist to prevent thermal conduction.^{19),20)}

Figure 5 shows the power factor (PF) of those samples. The PF of the Co-doped sample suddenly increases above the 740 K and gradually increase above 800 K. Since the conductivity of the Co-doped sample also suddenly increases at around same temperature as shown in Fig. 2, the conductivity change is responsible for this sudden change. However, the conductivity of the Co-doped sample doesn't change much above 800 K. There-

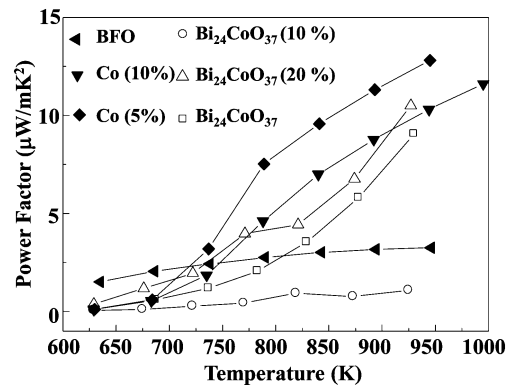


Fig. 5. Power factors of the Co-doped (0, 5, 10%) BiFeO_3 , $\text{Bi}_{24}\text{CoO}_{37}$ and $\text{Bi}_{24}\text{CoO}_{37}$ (10, 20%)–BFO composite system.

fore, change in the Seebeck coefficient is responsible for the PF of the Co-doped sample above 800 K. In addition to that, Co (5%) doped BFO showed the highest PF, which is about $12 \mu\text{W}/\text{mK}^2$ at 950 K. Although the PF became lower with the increase of Co content, it is still 5 times larger than that of non-doped BFO. On the other hand, the 20% composite sample also showed high PF compared with non-doped BFO. The composite sample and $\text{Bi}_{24}\text{CoO}_{37}$ has same temperature dependence of PF. This dependence is due to the conductivity change, because those samples showed 100 times changes in the conductivities within a measurement temperature as shown in Fig. 3.

4. Conclusions

We investigated thermoelectric properties of Co-doped BFO, the $\text{Bi}_{24}\text{CoO}_{37}$ and $\text{Bi}_{24}\text{CoO}_{37}$ –BFO composite system. XRD patterns revealed that all samples are identified as a Co-doped BFO, $\text{Bi}_{24}\text{CoO}_{37}$ and BFO– $\text{Bi}_{24}\text{CoO}_{37}$ composite. All sample showed positive sign in Seebeck coefficient, which means majority carrier of those samples is p-type. Most of samples showed high Seebeck coefficient above $400 \mu\text{V}/\text{K}$ except $\text{Bi}_{24}\text{CoO}_{37}$. On the other hand, $\text{Bi}_{24}\text{CoO}_{37}$ has the highest conductivity among the sample. From this results, BFO matrix play an important role for keeping high Seebeck coefficient and $\text{Bi}_{24}\text{CoO}_{37}$ works as a conductive pass on this system. Co (5%)–doped BFO and 20% composite sample showed high PF among the samples.

Acknowledgments This work was supported in part by a Grant-in-Aid for Young Scientists (A) (23686094) from the Japan Society for the Promotion of Science (JSPS) and the JSPS International Training Program (ITP), “Young Scientist-Training Program for World Ceramics Network”, and in part by a grant from the Institute of Ceramics Research and Education, NITECH.

References

- 1) I. Terasaki, Y. Sasago and K. Uchinokura, *Phys. Rev. B*, **56**, R12685–R12687 (1997).
- 2) I. Matsubara, Y. Zhou, T. Takeuchi, R. Funahashi, M. Shikano, N. Murayama, W. Shin and N. Izu, *J. Ceram. Soc. Japan*, **111**, 238–241 (2003).
- 3) S. Ohta, T. Nomura, H. Ohta and K. Koumoto, *J. Appl. Phys.*, **97**, 034106–034109 (2005).
- 4) T. Okuda, K. Nakanishi, S. Miyasaka and Y. Tokura, *Phys. Rev. B*, **63**, 113104–113107 (2001).
- 5) S. Ohta, H. Ohta and K. Koumoto, *J. Ceram. Soc. Japan*, **114**, 102–105 (2006).
- 6) W. Shin and N. Murayama, *Jpn. J. Appl. Phys.*, **38**, 1336–1338 (1999).

- 7) D. H. Flahaut, R. Funahashi, K. Lee, H. Ohta and K. Koumoto, International Conference on Thermoelectrics, ICT, Proceedings (2006) pp. 103–106.
- 8) P.-X. Thao, T. Tsuji and Y. Yamamura, *J. Ceram. Soc. Japan*, **112**, S663–S667 (2003).
- 9) S. Li, R. Funahashi, I. Matsubara, K. Ueno, S. Sodeoka and H. Yamada, *Chem. Mater.*, **12**, 2424–2427 (2000).
- 10) J. Seidel, L. W. Martin, Q. He, Q. Zhan, Y.-H. Chu, A. Rother, M. E. Hawkrige, P. Maksymovych, P. Yu, M. Gajek, N. Balke, S. V. Kalinin, S. Gemming, F. Wang, G. Catalan, J. F. Scott, N. A. Spaldin, J. Orenstein and R. Ramesh, *Nat. Mater.*, **8**, 229–234 (2009).
- 11) Ying-Hao Chu, Lane W. Martin, Mikel B. Holcomb, Martin Gajek, Shu-Jen Han, Qing He, Nina Balke, Chan-Ho Yang, Donkoun Lee, Wei Hu, Qian Zhan, Pei-Ling Yang, Arantxa Fraile-Rodríguez, Andreas Scholl, Shan X. Wang and R. Ramesh, *Nat. Mater.*, **7**, 478–482 (2008).
- 12) M. Shiga, *Bulletin of J. Inst. Metals.*, **17**, 582–588 (1978) [in Japanese].
- 13) M. Shiga and Y. Nakamura, *J. Phys. Soc. Jpn.*, **26**, 24–26 (1969).
- 14) I. S. Lyubutin, S. G. Ovchinnikov, A. G. Gavriliuk and V. V. Struzhkin, *Phys. Rev. B*, **79**, 085125 (2009).
- 15) R. D. Shanon, *Acta Crystallogr., Sect. A: Cryst. Phys., Diffr., Theor. Gen. Crystallogr.*, **32**, 751–767 (1976).
- 16) K. Oka, M. Azuma, W. Chen, H. Yusa, A. A. Belik, E. Takayama-Muromachi, M. Mizumaki, N. Ishimatsu, N. Hiraoka, M. Tsujimoto, M. G. Tucker, J. P. Attfield and Y. Shimakawa, *J. Am. Chem. Soc.*, **132**, 9438–9443 (2010).
- 17) M. Gomi, N. Nishimura and T. Yokota, *J. Appl. Phys.*, **101**, 09M109 (2007).
- 18) Z. Zhang, P. Wu, L. Chen and J. Wang, *Appl. Phys. Lett.*, **96**, 232906 (2010).
- 19) A. Glatz and I. S. Beloborodov, *Phys. Rev. B*, **79**, 041404 (2009).
- 20) A. Glatz and I. S. Beloborodov, *Phys. Rev. B*, **80**, 245440 (2009).